



OPEN

Biosynthesis of spinel nickel ferrite nanowhiskers and their biomedical applications

Hajar Q. Alijani^{1,2}, Siavash Irvani³, Shahram Pourseyedi^{1,2}✉, Masoud Torkzadeh-Mahani⁴, Mahmood Barani⁵ & Mehrdad Khatami^{6,7,8}✉

Greener methods for the synthesis of various nanostructures with well-organized characteristics and biomedical applicability have demonstrated several advantages, including simplicity, low toxicity, cost-effectiveness, and eco-friendliness. Spinel nickel ferrite (NiFe_2O_4) nanowhiskers with rod-like structures were synthesized using a simple and green method; these nanostructures were evaluated by X-ray diffraction analysis, transmission electron microscopy, scanning electron microscopy, and X-ray energy diffraction spectroscopy. Additionally, the prepared nanowhiskers could significantly reduce the survival of *Leishmania major* promastigotes, at a concentration of 500 $\mu\text{g/mL}$; the survival of promastigotes was reduced to $\approx 26\%$. According to the results obtained from MTT test (in vitro), it can be proposed that further studies should be conducted to evaluate anti-leishmaniasis activity of these types of nanowhiskers in animal models.

The nanowhiskers with unique shape, electrical, optical, magnetic, and surface properties have shown attractive clinical and biomedical potentials^{1,2}. Typically, the production of different nanostructures with well-organized morphologies and sizes is highly demanded by researchers and scientists due to their unique applications and properties^{3–7}.

Inorganic nanostructures with different mechanical and physical properties can be employed in different applications such as medicine, electronic device, sunscreens, military applications, photovoltaic cells, paints, catalysts, and among others^{8–16}. Among nanostructures, nanofibers are defined as structures with an outer diameter below 1000 nm^{17,18}. Nanowhisker is a type of nanofiber crystal with a diameter of less than 100 nm¹⁹. Nanowhiskers can have various applications in filtration^{20,21}, food packaging²², diagnosis²³, drug delivery²⁴, gene delivery^{25–27}, cancer therapy²⁸ and cell scaffolding²⁹.

In recent years, the mechanical properties and widespread applications of NiFe_2O_4 nanowhiskers have been demonstrated by researchers. Ferrites are ceramics made from a combination of iron oxide and divalent metals such as barium, strontium, lead, nickel, cobalt, among others^{30,31}. Ferrites have wide applications in various biomedical³², catalytic^{27,33–35}, wastewater³⁶, extraction³⁷, electrical³⁸ fields.

For the fabrication of nanowhiskers, various synthesis approaches have been reported, including microwave³⁹, carbo-thermal reduction⁴⁰, and electrospinning⁴¹ techniques. However, one of the important drawbacks with these methods is the dependence on expensive equipment or energy consumption, which is directly or indirectly a threat to environmental health⁴². To solve this problem, it is necessary to discover environmentally friendly production methods for the synthesis of nanostructures^{43–47}. Therefore, the green synthesis of nanostructures in various forms has been developed using plant extracts⁴⁸. The application of plant extracts for synthesizing nanostructures is in accordance with the principles of green chemistry. This bio-based method has some important advantages of low toxicity and eco-friendliness, and for the creation of nanostructures, plant extracts act as natural reducing⁴⁹ and stabilizing agents^{50–52}.

¹Department of Biotechnology, Shahid Bahonar University of Kerman, Kerman, Iran. ²Research and Technology Institute of Plant Production (RTIPP), Shahid Bahonar University of Kerman, Kerman, Iran. ³Faculty of Pharmacy and Pharmaceutical Sciences, Isfahan University of Medical Sciences, Isfahan, Iran. ⁴Biotechnology Department, Institute of Science and High Technology and Environmental Sciences, Graduate University of Advanced Technology, Kerman, Iran. ⁵Medical Mycology and Bacteriology Research Center, Kerman University of Medical Sciences, 7616913555 Kerman, Iran. ⁶Noncommunicable Diseases Research Center, Bam University of Medical Sciences, Bam, Iran. ⁷Department of Medical Biotechnology, Faculty of Medical Sciences, Tarbiat Modares University, Tehran, Iran. ⁸Cell Therapy and Regenerative Medicine Comprehensive Center, Kerman University of Medical Sciences, Kerman, Iran. ✉email: spseyedi@gmail.com; mehrdad7khatami@gmail.com

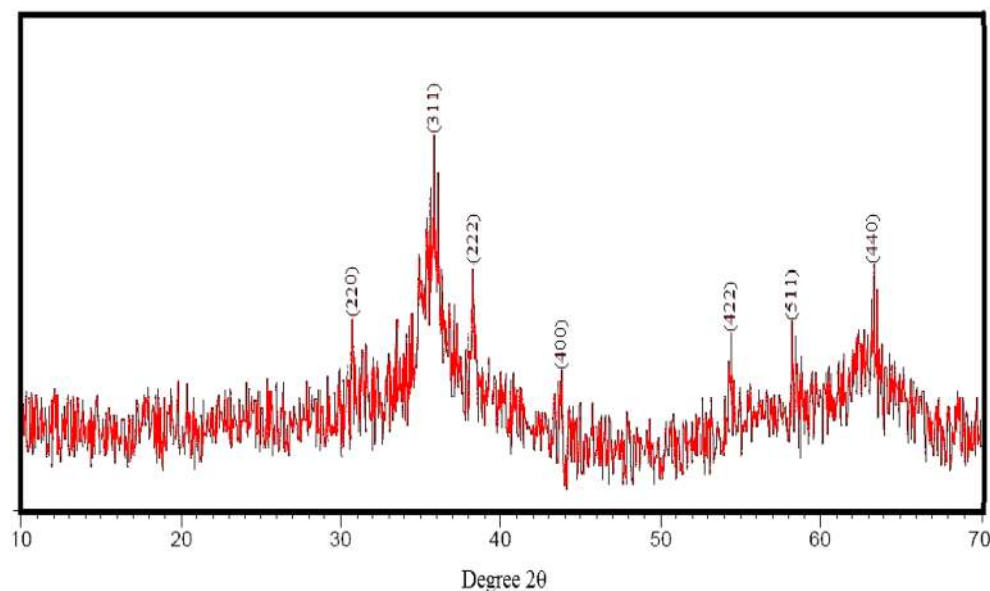


Figure 1. XRD pattern of the green-synthesized nickel-ferrite nanowhiskers.

As far as we know, no studies have been conducted for greener biosynthesis of spinel ferrite nanowhiskers; therefore, we focused on greener synthesis of spinel ferrite nanowhiskers using rosemary extract. Rosemary (*Rosmarinus officinalis*) is a woody, evergreen and fragrant medicinal plant, which contains phytochemicals such as rosmarinic acid, betulinic acid, camphor, carnosic acid, caffeic acid, carnosol, and ursolic acid. The active ingredients in rosemary have suitable antioxidant, anti-inflammatory, and antibacterial effects.

Aqueous extract of rosemary was utilized to make NiFe_2O_4 nanostructures in a single step at pH 7. X-ray powder diffraction (XRD), high-resolution transmission electron microscopy (HR-TEM), scanning electron microscopy (SEM), and energy-dispersive X-ray spectroscopy (EDX) techniques were employed to characterize these nanostructures. Additionally, antiparasitic activities of these nanostructures against *Leishmania major* were evaluated, in vitro.

Results

Characterization of NiFe_2O_4 nanowhiskers. The crystal and fuzzy structure of the synthesized nickel-ferrite nanostructures in the range $10\text{--}70^\circ$ is shown in Fig. 1. The peaks observed at 2θ correspond to the reverse spinel structure of nickel-ferrite nanostructures. The diffraction peaks correspond to lattice plane plates (220), (311), (222), (400), (422), (511), and (440)⁵³.

The structure of nickel-ferrite nanostructures is shown in HR-TEM image (Fig. 2, scale bar: 100 nm). According to the images, the surface of the synthesized nanostructures was smooth and even. The nanostructures were needle-like filaments (whiskers). Each hair-like strand has grown significantly in its longitudinal direction. Due to the presence of an interplate space of at least 10 nm, no aggregation or agglomeration of particles could be detected between hair-like strands such as NiFe_2O_4 nanowhiskers with soft surfaces. The size of these particles was less than 10 nm in width and more than 100 nm in length.

Figure 3a shows the surface morphology and number of constituents originated from NiFe_2O_4 nanowhiskers. As shown in SEM image, NiFe_2O_4 nanostructures are filamentous. The presence of nickel, oxygen and iron in the structure of the synthesized nanostructure was confirmed by EDX spectrum (Fig. 3b). EDX spectra demonstrated element ratios of Ni, Fe and O are 12, 24 and 48%, respectively.

Efficacy evaluation of nickel-ferrite nanowhiskers on *L. major*. The effectiveness of nickel-ferrite nanowhiskers with different concentrations for 48 h was evaluated based on MTT assay against *L. major* promastigotes (Fig. 4). Based on the obtained results, the survival rate of parasitic promastigotes was considerably lowered, when the concentration of nanostructures was increased. By applying nickel-ferrite nanowhiskers (with a concentration of 500 $\mu\text{g}/\text{ml}$), the survival of promastigotes was reduced to $\approx 26\%$, accordingly.

Nickel-ferrite nanowhiskers in a dose-dependent manner reduced the survival rate of *L. major* promastigotes, that when compared to the control group, this difference was statistically significant ($p < 0.05$). In MTT assay, IC_{50} on *L. major* promastigotes was about 100 $\mu\text{g}/\text{ml}$.

Discussion

Nickel-ferrite nanowhiskers were synthesized in one step using rosemary phenolic extract at minimal cost (Fig. 5).

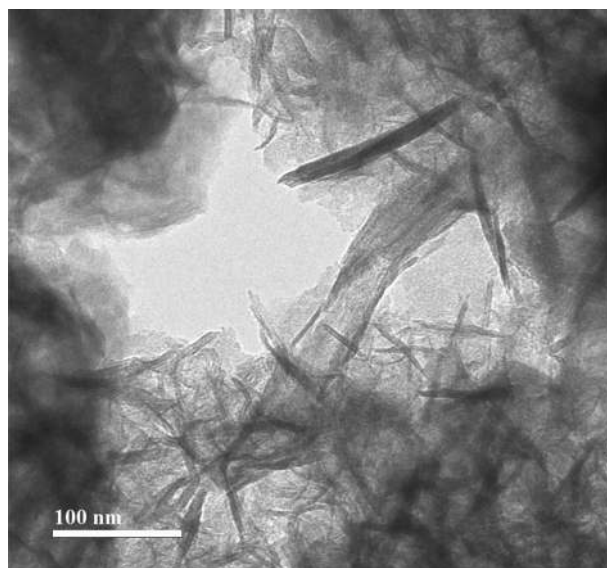


Figure 2. HR-TEM image of the green-synthesized nickel-ferrite nanowhiskers.

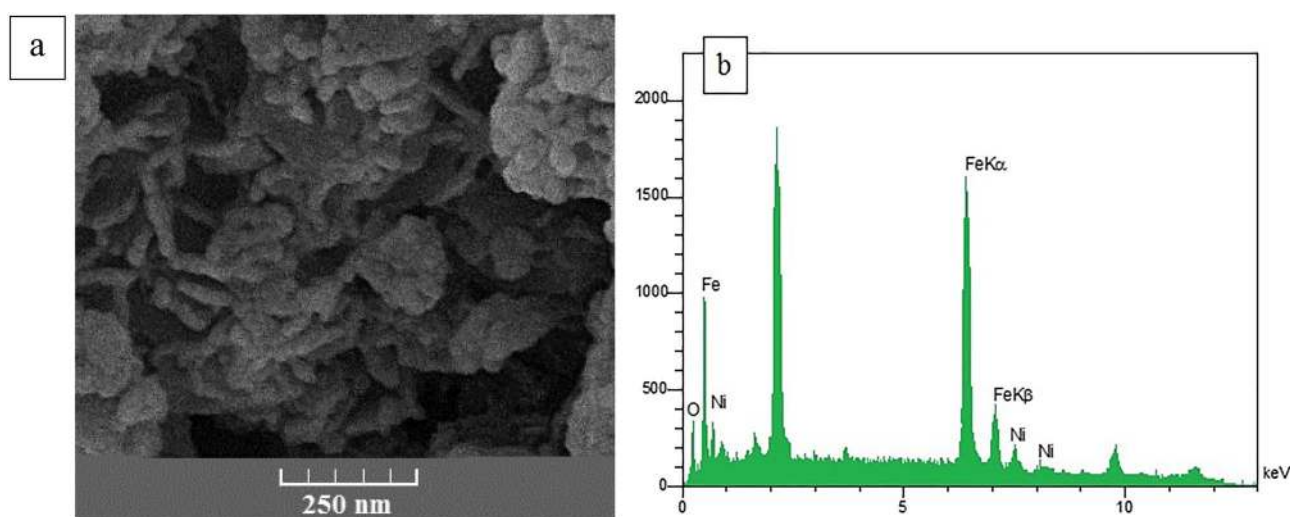


Figure 3. SEM and EDX images of green-synthesized nickel-ferrite nanowhiskers.

The cubic spinel structure of these spherical particles was identified by XRD analysis. Long strands of hair could be detected with a distinct morphologically margin of the whisker in HR-TEM.

Leishmaniasis is one of the most important infectious diseases in the world with 30,000 deaths annually⁵⁴, which leads to the death by damaging macrophage cells, spleen, bone marrow, and liver. With the advancement of technology and the inadequacy of current therapeutic drugs, the application of nanostructures with unique properties and plant extracts with antimicrobial activities has recently attracted the attention of researchers⁵⁵. Today, various nanostructures with different structures, suitable permeability, targeting properties, low toxicity, lack of resistance, high stability, and cost-effectiveness properties are widely deployed in the treatment of different diseases^{54,56}. The transfer of amphotericin to glycine polymer-coated iron oxide nanoparticles could significantly reduce *Leishmania* parasite in the spleen⁵⁷. Nickel oxide nanoparticles have anti-leishmaniasis activity against amastigotes and promastigotes of *Leishmania tropica* parasite⁵⁸. But to the best of our knowledge, there are no studies about leishmanicidal activity of nickel-ferrite nanowhiskers against *L. major* promastigotes.

Materials and methods

Greener synthesis of NiFe₂O₄ nanowhiskers. Rosemary leaves were collected from Kerman University Garden, Kerman, Iran. The rosemary leaves were collected in accordance with applicable institutional (Kerman University), national, and international rules and legislation. It was verified by the Iranian Botanical Survey, whose voucher specimen number was 1400/1 deposited at the Department Pharmacognosy, Kerman University.

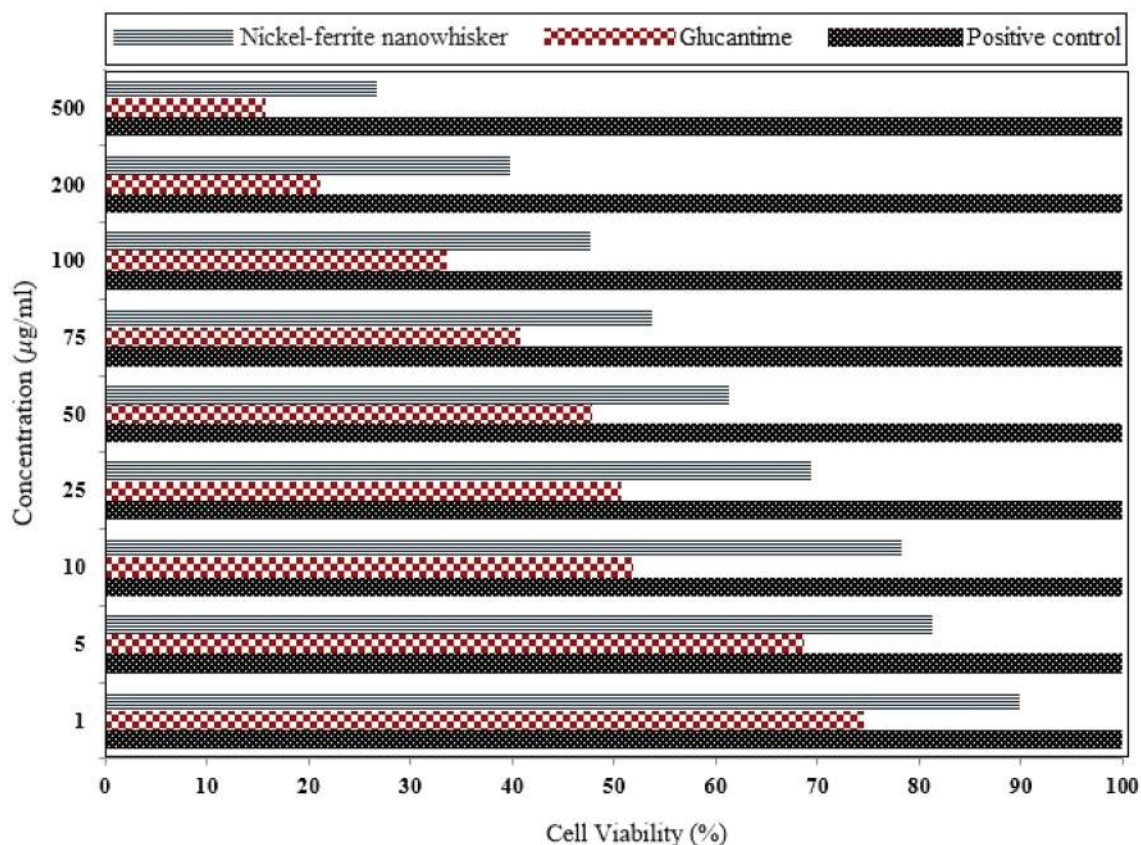


Figure 4. Survival percentage of *L. major* after 48 h of the exposure to different concentrations of nickel-ferrite nanowhiskers.

Fresh rosemary leaves were picked from the plant at the flowering stage. The leaves were disinfected using sodium hypochlorite for 3 min, and were washed 5 times with sterile deionized water and dried at 27 °C. 100 g of fresh rosemary leaves were warmed for one hour at 80 °C in 500 ml deionized water. In the next step, the mixture of leaves and deionized water was allowed to stand for one hour at room temperature and finally, filter paper was employed to separate the extract. To synthesize nickel-ferrite nanowhiskers, 1.7 g of iron (III) chloride ($\text{FeCl}_3 \cdot 6\text{H}_2\text{O}$, 98%, Merck) was dissolved on a heater at a temperature of 65–70 °C with 100 ml of aqueous rosemary extract by a strainer. 0.4 g of nickel chloride (II) ($\text{NiCl}_2 \cdot 6\text{H}_2\text{O}$, 99%, Merck) was added to the above mixture and dissolved at the same temperature by a strainer. Then, one molar solution of sodium carbonate (Na_2CO_3 anhydrous, $\geq 99.5\%$, Sigma-Aldrich) was added dropwise to bring the pH of the mixture to 10. Then, the mixture was stirred for about 3 h at 65–70 °C. The resulting nanostructures were separated through centrifuging, and then were washed with ethanol-deionized water and deionized water. Finally, these nanostructures were dried for 16 h at 60 degrees Celsius in an electric oven and ground into a soft powder⁵⁹.

Nickel-ferrite nanowhisker characterization. The crystal structure, morphology, and weight percentage of NiFe_2O_4 nanowhiskers were studied using XRD (X'PertPro, Panalytical; with Cu lamp), HRTEM (Sigma VP, ZEISS), and scanning electron microscope (SEM) coupled with energy-dispersive X-ray spectroscopy (EDX, TESCAN, Czech Republic).

Toxicity evaluation of nickel-ferrite nanowhiskers against *L. major*. The Center for Disease Control, Ministry of Health, in Iran, introduced Glucantime (meglumine antimoniate) as the chosen medicine for the treatment of all clinical types of leishmaniasis. Promastigotes of *L. major* were cultivated at 24 °C in a 25 ml flask with RPMI1640 (Roswell Park Memorial Institute media), 10% fetal bovine serum (FBS), and 2% penicillin and streptomycin. A colorimetric cell viability approach was deployed to quantify viable cells in micro-well plates to examine the impact of the produced nickel-ferrite nanowhiskers on *L. major* promastigotes. Tetrazolium has a positive charge and may easily permeate living cells, converting MTT from a soluble to an insoluble dye compound that this procedure called MTT assay. In brief, 100 µl of stationary phase promastigotes (5×10^4) cells/ml were introduced to a 96-well tissue culture plate. Following that, 100 µl of nickel-ferrite nanowhiskers (1, 5, 10, 25, 50, 75, 100, 200, and 500 µg/ml) were applied to each well and maintained for 48 h at 25 °C. Following the incubation period, 10 µl of MTT solution at concentration of 5 mg/ml was applied to each well and stored at 25 °C for 4 h. After that, cold isopropanol was utilized as a solvent for Formazan crystals, resulting in a purple colour. ELISA reader was employed to detect each well's absorption at 493 nm (BioTek-ELX800, Winooski, Vermont, USA). Promastigotes were cultured in drug-free RPMI1640 medium as control sample, and culture

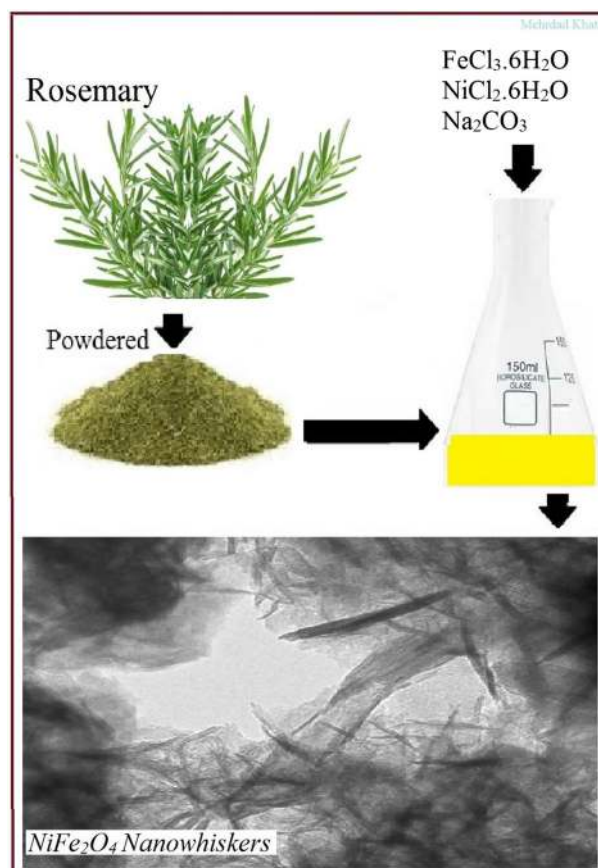


Figure 5. Schematic of nickel-ferrite nanowhiskers synthesis using rosemary extracts.

medium without promastigote and drug was also utilized as a pure sample. In SPSS software, the 50% inhibitory concentration or IC_{50} was computed for all concentrations studied using the Probit test.

Conclusion

In this study, nickel-ferrite nanowhiskers were eco-friendly synthesized using aqueous extract of rosemary. XRD, FESEM-EDAX, and HR-TEM evaluations confirmed the spinel and needle-like structures of the prepared nanostructures. Results obtained from in vitro studies revealed that the toxicity of nickel-ferrite nanowhiskers was improved against *L. major* promastigotes by increasing the concentration of nickel-ferrite nanowhiskers and treatment duration.

Received: 20 May 2021; Accepted: 18 August 2021

Published online: 31 August 2021

References

1. Fu, Z. *et al.* Shape control of Cu/ZnO core-shell nanocubes and related structures for localized surface plasmon resonance. *ACS Appl. Nano Mater.* **4**, 995–999 (2021).
2. Foroughi, M. M., Jahani, S. & Rajaei, M. Facile fabrication of 3D dandelion-like cobalt oxide nanoflowers and its functionalization in the first electrochemical sensing of oxymorphone: evaluation of kinetic parameters at the surface electrode. *J. Electrochem. Soc.* **166**, B1300–B1311. <https://doi.org/10.1149/2.0511914jes> (2019).
3. Nasrollahzadeh, M., Sajjadi, M., Irvani, S. & Varma, R. S. Trimetallic nanoparticles: greener synthesis and their applications. *Nanomaterials* **10**, 1784 (2020).
4. Raeisi, M. *et al.* Magnetic cobalt oxide nanosheets: green synthesis and in vitro cytotoxicity. *Bioprocess Biosyst. Eng.* **44**, 1423–1432 (2021).
5. Khatami, M., Zafarnia, N., Bami, M. H., Sharifi, I. & Singh, H. Antifungal and antibacterial activity of densely dispersed silver nanospheres with homogeneity size which synthesized using chicory: an in vitro study. *J. de Mycologie Médicale* **28** 637–644 (2018).
6. Mirzaei, H. *et al.* Direct growth of ternary copper nickel cobalt oxide nanowires as binder-free electrode on carbon cloth for nonenzymatic glucose sensing. *Microchem. J.* **142**, 343–351. <https://doi.org/10.1016/j.microc.2018.07.014> (2018).
7. Khatami, M. *et al.* Calcium carbonate nanowires: greener biosynthesis and their leishmanicidal activity. *RSC Adv.* **10**, 38063–38068. <https://doi.org/10.1039/D0RA04503A> (2020).
8. Dong, P. *et al.* Controllable synthesis of exceptionally small-sized superparamagnetic magnetite nanoparticles for ultrasensitive MR imaging and angiography. *J. Mater. Chem. B* **9**, 958–968 (2021).
9. Wang, Z. *et al.* Large-scale one-pot synthesis of water-soluble and biocompatible upconversion nanoparticles for dual-modal imaging. *Colloids Surf B Biointerfaces* **198**, 111480 (2021).

10. Chen, Z. *et al.* Fabrication of cellulosic paper containing zeolitic imidazolate framework and its application in removal of anionic dye from aqueous solution. *BioResources* **16** 2644–2654 (2021).
11. Hesaraki, M. *et al.* Knowledge, attitude, practice and clinical recommendations of health care workers towards COVID-19: a systematic review. *Review. Environm.l Health* **35**, 1–13 (2020).
12. Dai, Z., Guo, S., Gong, Y. & Wang, Z. Semiconductor flexoelectricity in graphite-doped SrTiO₃ ceramics. *Ceram. Int.* **47**, 6535–6539 (2021).
13. Safaei, M. *et al.* A review on metal-organic frameworks: Synthesis and applications. *TrAC Trend. Analytic. Chem* **118**, 401–425 (2019).
14. Rabiee, N. *et al.* Diatoms with invaluable applications in nanotechnology, biotechnology, and biomedicine: recent advances. *ACS Biomater. Sci. Eng.* <https://doi.org/10.1021/acsbiomaterials.1c00475> (2021).
15. Sargazi, S. *et al.* Synthesis, characterization, toxicity and morphology assessments of newly prepared microemulsion systems for delivery of valproic acid. *J. Mol. Liq.* **338**, 116625. <https://doi.org/10.1016/j.molliq.2021.116625> (2021).
16. Sabouri, Z., Akbari, A., Hosseini, H. A., Khatami, M. & Darroudi, M. Egg white-mediated green synthesis of NiO nanoparticles and study of their cytotoxicity and photocatalytic activity. *Polyhedron* **178**, 114351. <https://doi.org/10.1016/j.poly.2020.114351> (2020).
17. VillaVelázquez-Mendoza, C. I. *et al.* Simultaneous synthesis of β-Si₃N₄ nanofibers and pea-pods and hand-fan like Si₂N₂O nanostructures by the CVD method. *Mater. Lett.* **175**, 139–142. <https://doi.org/10.1016/j.matlet.2016.04.028> (2016).
18. Guo, J., Gao, J., Xiao, C., Chen, L. & Qian, L. Mechanochemical reactions of GaN-Al₂O₃ interface at the nanoasperity contact: roles of crystallographic polarity and ambient humidity. *Friction* **2021**, 1–14 (2021).
19. Dolete, G., Ilie, C. E., Nicoară, I. F., Vlăsceanu, G. M. & Grumezescu, A. M. in *Nanobiomaterials in Dentistry* (ed Alexandru Mihai Grumezescu) 27–47 (William Andrew Publishing, 2016).
20. Gopi, S., Kargl, R., Kleinschek, K. S., Pius, A. & Thomas, S. Chitin nanowhisker-Inspired electrospun PVDF membrane for enhanced oil-water separation. *J. Environ. Manage.* **228**, 249–259 (2018).
21. Liu, M., Xue, Z., Zhang, H. & Li, Y. Dual-channel membrane capacitive deionization based on asymmetric ion adsorption for continuous water desalination. *Electrochem. Commun.* **125**, 106974 (2021).
22. Haghghi, H. *et al.* Characterization of bio-nanocomposite films based on gelatin/polyvinyl alcohol blend reinforced with bacterial cellulose nanowhiskers for food packaging applications. *Food Hydrocolloids* **113**, 106454 (2021).
23. Tang, H. *et al.* High-strength paper enhanced by chitin nanowhiskers and its potential bioassay applications. *Int. J. Biol. Macromol.* **150**, 885–893 (2020).
24. Dash, R. & Ragauskas, A. J. Synthesis of a novel cellulose nanowhisker-based drug delivery system. *RSC Adv.* **2**, 3403–3409 (2012).
25. Zou, Q., Xing, P., Wei, L. & Liu, B. Gene2vec: gene subsequence embedding for prediction of mammalian N⁶-methyladenosine sites from mRNA. *RNA* **25**, 205–218 (2019).
26. Zhao, H. *et al.* Comprehensive landscape of epigenetic-dysregulated lncRNAs reveals a profound role of enhancers in carcinogenesis in BC subtypes. *Mol. Therapy-Nucleic Acids* **23**, 667–681 (2021).
27. Rahimi, S., Poormohammadi, A., Salmani, B., Ahmadian, M. & Rezaei, M. Comparing the photocatalytic process efficiency using batch and tubular reactors in removal of methylene blue dye and COD from simulated textile wastewater. *Journal of Water Reuse and Desalination* **6**, 574–582. <https://doi.org/10.2166/wrd.2016.190> (2016).
28. Xu, J. *et al.* UBQLN1 mediates sorafenib resistance through regulating mitochondrial biogenesis and ROS homeostasis by targeting PGC1β in hepatocellular carcinoma. *Signal Transduct. Target. Ther.* **6**, 1–13 (2021).
29. Krishnan, V. *et al.* Vortex-aligned fullerene nanowhiskers as a scaffold for orienting cell growth. *ACS Appl. Mater. Interfaces.* **7**, 15667–15673 (2015).
30. Vedrtam, A., Kalauni, K., Dubey, S. & Kumar, A. A comprehensive study on structure, properties, synthesis and characterization of ferrites. *AIMS Mater. Sci.* **7**, 800–835 (2020).
31. Ordoukhanian, J., Nezhadali, A. & Mehri, L. Electrosynthesis of Co, Ni and Zn ferrites nanoparticles in the presence of external magnetic field. *Ceram. Int.* **47**, 16841–16844 (2021).
32. Amiri, M., Salavati-Niasari, M. & Akbari, A. Magnetic nanocarriers: evolution of spinel ferrites for medical applications. *Adv. Coll. Interface. Sci.* **265**, 29–44 (2019).
33. Patil, S., Naik, H. B., Nagaraju, G., Viswanath, R. & Rashmi, S. Sugarcane juice mediated eco-friendly synthesis of visible light active zinc ferrite nanoparticles: application to degradation of mixed dyes and antibacterial activities. *Mater. Chem. Phys.* **212**, 351–362 (2018).
34. Malakotian, M. *et al.* Protocol encompassing ultrasound/Fe₃O₄ nanoparticles/persulfate for the removal of tetracycline antibiotics from aqueous environments. *Clean Technol. Environ. Policy* **21**, 1665–1674. <https://doi.org/10.1007/s10098-019-01733-w> (2019).
35. Seid-Mohammadi, A., Gh, A., Sammadi, M., Ahmadian, M. & Poormohammadi, A. Removal of humic acid from synthetic water using chitosan as coagulant aid in electrocoagulation process for Al and Fe electrodes. *Res. J. Chem. Environ* **18**, 5 (2014).
36. Kefeni, K. K., Mamba, B. B. & Msagati, T. A. Application of spinel ferrite nanoparticles in water and wastewater treatment: a review. *Sep. Purif. Technol.* **188**, 399–422 (2017).
37. Xia, S. *et al.* Preparation of porous zinc ferrite/carbon as a magnetic-assisted dispersive miniaturized solid phase extraction sorbent and its application. *J. Chromatogr. A* **1567**, 73–80 (2018).
38. Hussain, K., Amin, N. & Arshad, M. I. Evaluation of structural, optical, dielectric, electrical, and magnetic properties of Ce³⁺-doped Cu_{0.5}Cd_{0.25}Co_{0.25}Fe_{2-x}O₄ spinel nano-ferrites. *Ceramics Int.* **47**, 3401–3410 (2021).
39. Lee, C., Kahar, S. & Voon, C. Microwave synthesis of silicon carbide nanowhiskers: Effect of molar ratio. *Mater. Today Proc.* **37**, 119–121 (2021).
40. Lao, X., Xu, X., Jiang, W., Liang, J. & Miao, L. Influences of Al metal and Al–Si alloys on in-situ synthesis of SiC nanowhiskers in porous Al₂O₃–SiC composites obtained by carbothermal reduction. *J. Alloys Compd.* **854**, 157182 (2021).
41. Ghadimi, Z., Esfahani, H. & Mazaheri, Y. Control on nanostructured quaternary Ti–Al–O–B composite synthesized via electro-spinning method, from nanoparticles to nanowhiskers. *J. Sol-Gel. Sci. Technol.* **98**, 127–137 (2021).
42. Ma, M.-G., Dong, Y.-Y., Fu, L.-H., Li, S.-M. & Sun, R.-C. Cellulose/CaCO₃ nanocomposites: microwave ionic liquid synthesis, characterization, and biological activity. *Carbohydr. Polym.* **92**, 1669–1676 (2013).
43. Yılmaz Öztürk, B., Yenice Gürsu, B. & Dağ, İ. Antibiofilm and antimicrobial activities of green synthesized silver nanoparticles using marine red algae Gelidium corneum. *Process Biochem.* **89**, 208–219 (2020).
44. Raessi, M. *et al.* Barium carbonate nanostructures: Biosynthesis and their biomedical applications. *Ceram. Int.* <https://doi.org/10.1016/j.ceramint.2021.04.106> (2021).
45. Mohammadinejad, R., Karimi, S., Iravani, S. & Varma, R. S. Plant-derived nanostructures: types and applications. *Green Chem.* **18**, 20–52. <https://doi.org/10.1039/C5GC01403D> (2016).
46. Sun, M. *et al.* Effects of NaClO shock on MBR performance under continuous operating conditions. *Environ. Sci.: Water Res. Technol.* **7**, 396–404 (2021).
47. Zhang, L. *et al.* Effect of Fe³⁺ on the sludge properties and microbial community structure in a lab-scale A₂O process. *Sci. Total Environ.* **780**, 146505 (2021).
48. Hamidian, K., Saberian, M. R., Miri, A., Sharifi, F. & Sarani, M. Doped and un-doped cerium oxide nanoparticles: biosynthesis, characterization, and cytotoxic study. *Ceram. Int.* **47**, 13895–13902. <https://doi.org/10.1016/j.ceramint.2021.01.256> (2021).

49. Azhdari, S. *et al.* Metallic SPIONP/AgNP synthesis using a novel natural source and their antifungal activities. *RSC Adv.* **10**, 29737–29744 (2020).
50. Khatami, M. *et al.* Greener synthesis of rod shaped zinc oxide nanoparticles using lilium ledebourii tuber and evaluation of their leishmanicidal activity. *Iran. J. Biotechnol.* **18**, e2196–e2196. <https://doi.org/10.30498/IJB.2020.119481.2196> (2020).
51. Alinaghi Langari, A. *et al.* CeO₂ foam-like nanostructure: biosynthesis and their efficient removal of hazardous dye. *Bioprocess Biosyst. Eng.* **44**, 517–523. <https://doi.org/10.1007/s00449-020-02464-9> (2021).
52. Khatami, M. *et al.* Simplification of gold nanoparticle synthesis with low cytotoxicity using a greener approach: opening up new possibilities. *RSC Adv.* **11**, 3288–3294. <https://doi.org/10.1039/D0RA08822F> (2021).
53. Mirgorod, Y. A., Borshch, N. A., Fedosyuk, V. M. & Yurkov, G. Y. Magnetic properties of nickel ferrite nanoparticles prepared using flotation extraction. *Inorg. Mater.* **49**, 109–114. <https://doi.org/10.1134/S0020168512110064> (2013).
54. Nafari, A. *et al.* Nanoparticles: New agents toward treatment of leishmaniasis. *arasite epidemiology and control*, **10**, e00156 (2020).
55. Guo, J. *et al.* Interplay between counter-surface chemistry and mechanical activation in mechanochemical removal of N-faced GaN surface in humid ambient. *Tribol. Int.* **159**, 107004 (2021).
56. Rahdar, A. *et al.* Deferasirox-loaded pluronic nanomicelles: Synthesis, characterization, in vitro and in vivo studies. *J. Mol. Liquids* **323**, 114605 (2021).
57. Kumar, R. *et al.* Development of high efficacy peptide coated iron oxide nanoparticles encapsulated amphotericin B drug delivery system against visceral leishmaniasis. *Mater. Sci. Eng., C* **75**, 1465–1471 (2017).
58. Iqbal, J. *et al.* Green synthesis and characterizations of Nickel oxide nanoparticles using leaf extract of Rhamnus virgata and their potential biological applications. *Appl. Organometal. Chem.* **33**, e4950 (2019).
59. Alijani, H. Q., Pourseyedi, S., Torkzadeh-Mahani, M., Seifalian, A. & Khatami, M. Bimetallic nickel-ferrite nanorod particles: greener synthesis using rosemary and its biomedical efficiency. *Artif. Cells Nanomed. Biotechnol.* **48**, 242–251. <https://doi.org/10.1080/21691401.2019.1699830> (2020).

Acknowledgements

This research was carried out using the funding and support of Research and Technology Institute of Plant Production of Shahid Bahonar University of Kerman, Iran. Also was supported by the VEGA Agency under the Contract no. 2/0140/20 and Bam University of Medical Sciences (M. Khatami grant No. 1400/018), Electron microscopy at the Institute of Macromolecular Chemistry was supported through Grants 17-05007S (Czech Science Foundation) and POLYMAT LO1507 (Ministry of Education, Youth and Sports of the CR, program NPU I).

Author contributions

Pourseyedi, SH. Barani, M. and Khatami, M. wrote the main manuscript text and Iravani, S. and Alijani, H prepared figures 1-3. All authors reviewed the manuscript.

Competing interests

The authors declare no competing interests.

Additional information

Correspondence and requests for materials should be addressed to S.P. or M.K.

Reprints and permissions information is available at www.nature.com/reprints.

Publisher's note Springer Nature remains neutral with regard to jurisdictional claims in published maps and institutional affiliations.



Open Access This article is licensed under a Creative Commons Attribution 4.0 International License, which permits use, sharing, adaptation, distribution and reproduction in any medium or format, as long as you give appropriate credit to the original author(s) and the source, provide a link to the Creative Commons licence, and indicate if changes were made. The images or other third party material in this article are included in the article's Creative Commons licence, unless indicated otherwise in a credit line to the material. If material is not included in the article's Creative Commons licence and your intended use is not permitted by statutory regulation or exceeds the permitted use, you will need to obtain permission directly from the copyright holder. To view a copy of this licence, visit <http://creativecommons.org/licenses/by/4.0/>.

© The Author(s) 2021